Grenze International Journal of Engineering and Technology, Jan Issue

Highly Isolated Hexagonal Shaped DGS based MIMO Antenna for C-Band Applications

Praveen Kumar[1], Rashmi Sinha[2], Arvind Choubey[3], Santosh Kumar Mahto[4], Pravesh Pal[5], Ranjeet Kumar[6] and Ajit Kumar Singh[7]
[1-2, 5-6]National Institution of Technology / Department of Electronics & Communication Engineering, Jamshedpur, India
Email: 2018rsec005@nitjsr.ac.in, rsinha.ece@nitjsr.ac.in, praveshpal9@gmail.com, ranjeet77kumar@gmail.com
[3]Indian Institute of Information Technology / Department of Electronics & Communication Engineering, Bhagalpur, India
Email: achoubey.ece@nitjsr.ac.in
[4, 7]Indian Institute of Information Technology / Department of Electronics & Communication Engineering, Ranchi, India
Email: skumar@iiitranchi.ac.in, ajitsingh31393@gmail.com

***Abstract*—In this article, we present a miniaturized wideband multiple-input multiple-output antenna with high isolation for C band use. It consists of 2×1 hexagonal motifs which serves as radiating elements. Defected ground structure (DGS) technique is employed to attain an efficient isolation between the antenna elements. Two inverted L-shaped stubs are incorporated to enhance the isolation and reduce the antenna size enlargement simultaneously, by suppressing the surface waves. The overall dimension of the designed MIMO antenna is 30 × 20 mm^2. The proposed DGS structure provides - 40.81 dB of isolation at 7.88 GHz and a gap of 4 mm between adjacent antenna elements. Envelope correlation coefficient (ECC) is less than 0.01, diversity gain (DG) greater than 9.95 dB, total active reflection coefficient (TARC) less than 0.4, mean effective gain (MEG) less than -3 dB, and channel capacity loss (CCL) less than 0.4 is achieved. Besides, scattering matrix such as return loss S_{11} and transmission coefficient S_{21} between two elements, radiation pattern, and current distribution was also favorable for C-band and X-band applications.**

***Index Terms*— DGS, ECC, Isolation, Mutual coupling, MIMO.**

I. Introduction

MIMO Antenna can achieve the requirement for high data rate transfer in current and future generations over the Communication channels. MIMO antenna is characterized by high channel capacity [1], robustness of the communication link [2], high data rate [3], and spectral efficiency [4]. It usually requires a very small distance between adjacent antenna elements to achieve compact size. The main challenge to design a MIMO antenna is the trade-off between closely packed and isolation between adjacent antennas. MIMO systems are affected by high mutual coupling due to the compactness of the terminals. The interference between two antennas is mutual coupling, which deteriorates the antenna's radiation characteristics [5], channel capacity, bandwidth, and efficiency [6]. Hence, isolation between different antenna elements is the main factor that needs to be taken care of and maintained as high as possible. It is possible to improve isolation by increasing separation of antennas by a distance more than λ/2. However, achieving such a compact antenna is not feasible.
There are several isolation enhancement techniques present in literature to overcome the above problem, such as

Grenze ID: 01.GIJET.9.1.524_2

split ring resonator (SRR) [7], parasitic element [8], decoupling networks [9], electromagnetic band gap structure (EBG) [10,11], DGS [12–14] etc. However, EBG structure is complex in design and larger in size due to its periodic structure. For all the isolation enhancement techniques listed previously, DGS is the simplest and least complex to fabricate. It is executed by etching different types of shapes on the ground, for increasing isolation between adjacent antenna [15–21].

A DGS is identical to a resonance LC circuit, which behaves like a stopband filter. This stopband filter is used to stop the surface wave between different antennas in the desired frequency range, thereby improving isolation between antenna elements.

In this paper, we introduce two closely placed hexagonal shape patch antenna. Two simple inverted L-shaped patterns are incised on the bottom to introduce DGS, which acts as a resonant slot and enhances the isolation. The gap between the adjacent antennas is significantly reduced by 4 mm. Maximum isolation of -40.81 dB at 7.88 GHz is achieved. This antenna has a miniaturized size 30 × 20 mm^2 and frequency band ranging from 4.33 to 10.1 GHz, which is applicable for C-band and a few lower X-band applications.

II. PROPOSED ANTENNA DESIGN

In this segment, we introduce the layout procedure of the designed MIMO system with the DGS technique. The development of the novel MIMO system is completed in two sequential stages as shown in Figure 1. Two hexagonal motifs are presented on the substrate in the first step, which serves as radiating elements. In the second stage shown in Figure 1(b), two inverted L-shaped stub isolators are incorporated on the ground. This stub isolator is proposed after investigating a number of structures available abundantly, which could enhance the isolation. The final MIMO antenna is printed on an inexpensive FR-4 lossy substrate with a thickness of 1.6 mm, dielectric constant (ε_r) = 4.3, and loss-tangent (δ) = 0.025 shown in figure 1 (c). Simulation has been achieved with the use of HFSS 19.0. The optimized layout characteristics for the MIMO antenna and inverted L-shaped stub are L=30 mm, W=20 mm, SW=1 mm, T=0.4 mm, G=0.5 mm, FL=6 mm ,GW=4 mm, SL=6 mm, R=5.73 mm, and FW=1.75 mm.

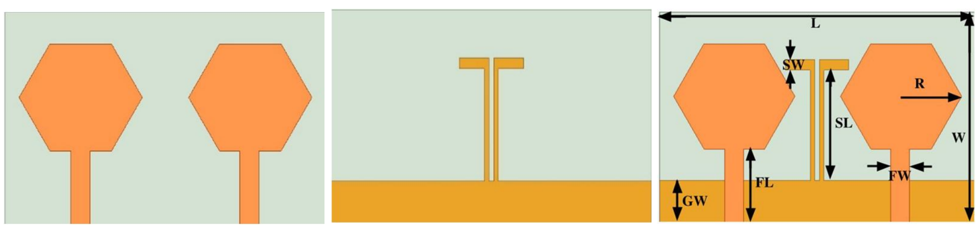

(a) (b) (c)

Figure 1: Simulated (a) top view, (b) bottom view, and (c) the proposed MIMO antenna

III. SIMULATION AND PERFORMANCE ANALYSIS

The overall performance of the designed MIMO antenna is analysed by evaluating S-parameter, radiation pattern, and diversity performance consisting of MEG, ECC, DG, TARC, and CCL are also presented in this section.

Figure 2 shows simulated reflection (S_{11}) and transmission (S_{12}) coefficients of a designed MIMO antenna with and without stubs. Across the entire bandwidth, the S_{11} and S_{12} are less than -10 dB, and -15 dB, respectively, and are less than -10 dB, and respectively, without stubs. The peak isolation is -40.81 dB at 7.88 GHz. The enhanced isolation achieved with an inverted L-shaped stub is 29.31 dB at 7.88 GHz. The peak value of S12 with and without inverted L-shaped stub is -40.81 dB at 7.88 GHz and -26.83 dB at 5.0 GHz respectively. The desired impedance bandwidth of 5.77 GHz with a range of 4.33 to 10.1 GHz is achieved. Figure 2 illustrates that an isolator reduces bandwidth while increasing isolation between adjacent antennas.

Figure 3 represents 2D radiation pattern of the designed two port MIMO antenna at 5.3 GHz and it is noticed that at ϕ = 0°, pattern is similar to a dipole and omnidirectional at ϕ = 90°.

Diversity characteristics such as ECC, DG, MEG, TARC, and CCL are considered to verify the designed MIMO antenna's performance and capability.

Mutual coupling and correlation between two radiators are calculated using ECC. It can be calculated using equation (1) [22] which is only valid for lossless equally transmitted energy through antennas. Therefore, it produces a fictitious result that is different from the actual result. The value of ECC is therefore computed by

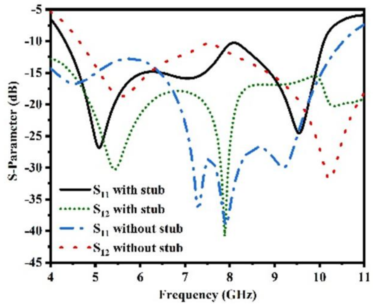

Figure 2: S-parameter characteristics

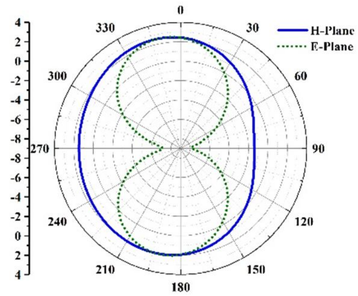

Figure 3: 2-D radiation pattern

equation (2) based on the radiated fields. Equation (2) can be used for calculating the real diversity performance of ECC.

$$ECC = \frac{|S_{11}^{*}S_{12}+S_{21}^{*}S_{22}|^2}{(1-|S_{11}|^2-|S_{21}|^2)(1-|S_{22}|^2-|S_{12}|^2)} \quad (1)$$

As shown in Figure 4, the ECC of the proposed MIMO antenna is less than 0.01. The ECC should ideally be zero, but in practice less than 0.5 is acceptable. The real diversity performance of ECC can be calculated using equation (2).

$$ECC = \frac{|\iint_{4\pi} R_1^{*}(\theta,\varphi).R_2(\theta,\varphi)\,d\Omega|^2}{\iint_{4\pi}|R_1(\theta,\varphi)|^2 d\Omega \times \iint_{4\pi}|R_2(\theta,\varphi)|^2 d\Omega} \quad (2)$$

where R_1 and R_2 are the radiated fields of antenna elements 1 & 2, ϕ, θ and Ω are the azimuthal, elevation and solid angles respectively.
In a MIMO system, DG can also be used to measure the reduction in transmission power due to DGS. The DG can be calculated by equation (3) [23].

$$DG = \sqrt{1-(ECC)^2} \quad (3)$$

Figure 4 shows that the DG of the design MIMO system is greater than 9.95 dB. This value approaches the ideal value (≈10 dB) suggesting that diversity performance is good.

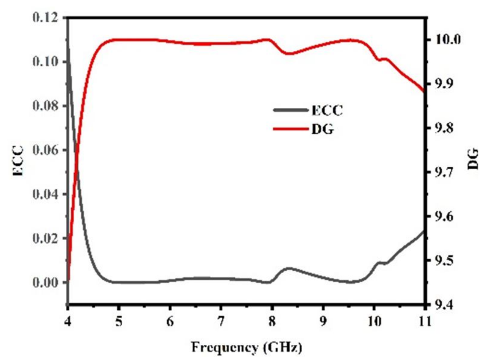

Figure 4: ECC and DG of the design antenna

During the simultaneous operation of two antenna elements, contiguous antennas are in direct contact. As a result, the overall gain, bandwidth, and efficiency are affected. Due to this issue, S-parameters alone cannot predict the performance of the MIMO antenna, so the TARC must be taken into account for this effect.

$$TARC = \frac{\sqrt{\sum_{i=1}^{n}|b_i|^2}}{\sqrt{\sum_{i=1}^{n}|a_i|^2}} \quad (4)$$

where a_i and b_i are incident and reflected power respectively.
S-parameter is also used to calculate the TARC value of the dual-port antenna (5) [24].

$$TARC = \sqrt{\frac{(S_{11}+S_{12})^2+(S_{21}+S_{22})^2}{2}} \tag{5}$$

The real value of TARC varies between 0 to 1. In case the value of TARC is zero, all power will be transmitted, while when TARC is one, all the power will be bounced back or transferred to nearby ports. The value of TARC is less than 0.4 in the operating band as shown in Figure 5.

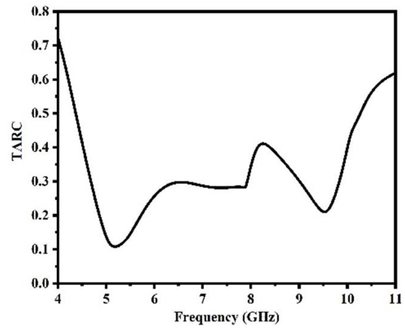

Figure 5: TARC of the design antenna

Another diversity parameter is TARC, which describes how antennas impact channel budgets. In a hazing climate, MEG_i is determined by equations (6) and (7) [24].

$$MEG_i = 0.5[1 - \sum_{j=1}^{N} |S_{ij}|^2] < -3\ dB \tag{6}$$

$$MEG_j = 0.5[1 - \sum_{i=1}^{N} |S_{ji}|^2] < -3\ dB \tag{7}$$

$$|MEG_i - MEG_j| < 3\ dB \tag{8}$$

$$|MEG_i / MEG_j| = \pm 3\ dB \tag{9}$$

where i, j serves as antenna 1 and 2 individually. Figure 10 illustrate the MEG*i*, which is less than -3 dB for the desired frequency range. Hence, the design antenna performs well in terms of diversity.

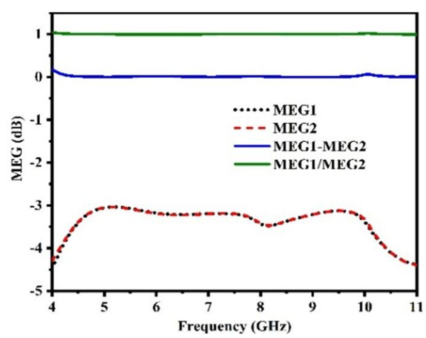

Figure 6: MEG of the deigned antenna

The performance of the MIMO antenna is decisive by its channel capacity. As the number of antenna increases, MIMO antenna capacity increases. However, as the correlation factor between antennas increases, channel capacity loss (CCL) also increases. CCL can be calculate with the help of of Equation (10).

$$CCL = -log_2 \det[\beta^2] \tag{10}$$

Where,

$$[\beta^2] = \begin{bmatrix} \beta_{ii} & \beta_{ij} \\ \beta_{ji} & \beta_{jj} \end{bmatrix} \tag{11}$$

$$\beta_{ii} = 1 - (\sum_{j=1}^{N} |S_{ij}|^2) \tag{12}$$

$$\beta_{ij} = 1 - (S_{ii}^{*}S_{ij} + S_{ji}^{*}S_{jj}) \quad (13)$$

Figure 7 shows that the value of CCL is less than 0.3 bit/s/Hz. Which is less than the ideal value (0.4 bit/s/Hz) exhibiting good diversity performance.

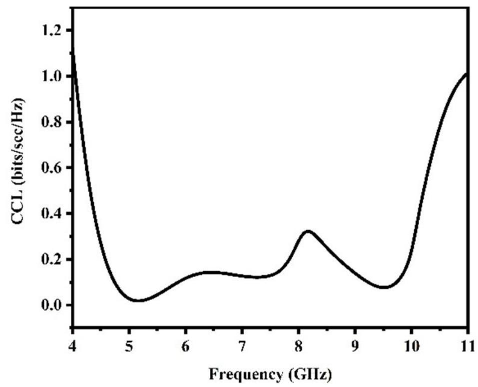

Figure 7: CCL of the designed antenna

Table I compares the designed work with related works that have recently been published, and the results are summarized. The size of this designed antenna is 30×20 mm^2, making it more compact than all others. However, the ECC of [9,19,25,26,27] is larger and isolation is weaker compared to this work except [25,30]. [25,30] has a larger distance between adjacent antenna's edges and higher isolation than the proposed work. The proposed work is more isolated than any of the other antennas reported in Table 1. Larger bandwidth is claimed in [19] but at the cost of poor isolation and high ECC value. [29,30] has low ECC, large dimension. Hence, the proposed inverted L-shaped stub-based DGS technique can be seen as a useful commercially usable tool to achieve efficient isolation in a MIMO antenna. It does not disturb the primary radiation mode. It can be preferably applicable for C-band applications such as developing new generation air-borne and space-borne radars.

TABLE I. COMPARISON OF THE PROPOSED WITH RECENT WORKS

Ref.	Dimension (mm^2)	Bandwidth (GHz)	Edge to edge gap (mm)	Max. Isolation (dB)	ECC
[9]	78×40	2.4-6.55	10	-35	0.1
[19]	32×32	3.1-10.6	-	-30	0.02
[25]	50×30	2.5–14.5	-	-50	0.04
[26]	75×150	3.3-5.0	10	-40	0.05
[27]	80×80	5.71-8.2	23.29	-25	0.05
[28]	66×66	1.8-2.6	31.84	-40	0.01
[29]	50×22.5	5.23-6.42	12.2	-40	0.001
[30]	97×27.69	5.4–6.0	13.75	-43	0.005
This work	30×20	4.33-10.1	4	-40.81	0.01

IV. CONCLUSION

The designed MIMO antenna with two inverted L-shaped Stub is small, inexpensive, and easy to construct. There is a small gap of 4 mm between the edges of the antenna, providing the required frequency range from 4.33 to 10.1 GHz. Two simple L-shaped stubs have been included to achieve high isolation in desired frequency band. Maximum isolation is -40.81 dB at 7.88 GHz without deteriorating the bandwidth. This antenna exhibits good performance parameters within the desired frequency range and therefore its application in C band can be envisaged.

REFERENCES

[1] S. Chouhan, D. K. Panda, M. Gupta, and S. Singhal. Meander line mimo antenna for 5.8 ghz wlan application. *International Journal of RF and Microwave Computer-Aided Engineering*, 28(4):e21222, (2018).

[2] Constantine A Balanis. *Antenna theory: analysis and design*. John wiley & sons, 2015.

[3] P. Beigi, M. Rezvani, Y. Zehforoosh, J. Nourinia, and B. Heydarpanah. A tiny ebg-based structure multiband mimo antenna with high isolation for lte/wlan and c/x bands applications. *International Journal of RF and Microwave Computer-Aided Engineering*, 30(3):e22104, (2020).
[4] D. Tse and P. Viswanath. *Fundamentals of wireless communication*. Cambridge university press, (2005).
[5] M. Alibakhshikenari, B. S. Virdee, P. Shukla, C. H. See, Raed A Abd-Alhameed, Francisco Falcone, Karim Quazzane, and Ernesto Limiti. Isolation enhancement of densely packed array antennas with periodic mtm-photonic bandgap for sar and mimo systems. *IET Microwaves, Antennas & Propagation*, 14(3):183–188, 2020.
[6] H. Li, Y. Tan, B. K. Lau, Z. Ying, and S. He. Characteristic mode based tradeoff analysis of antenna-chassis interactions for multiple antenna terminals. *IEEE Transactions on Antennas and Propagation*, 60(2):490–502, 2011.
[7] Li L, Zhou ZL, Hong JS, Wang BZ. Compact dual-band-notched UWB planar monopole antenna with modified SRR. Electronics Letters. 2011;47(17):950-1.
[8] Jiang W, Che W. A novel UWB antenna with dual notched bands for WiMAX and WLAN applications. IEEE Antennas and Wireless Propagation Letters. 2012;11:293-6.
[9] Banerjee J, Karmakar A, Ghatak R, Poddar DR. Compact CPW-fed UWB MIMO antenna with a novel modified Minkowski fractal defected ground structure (DGS) for high isolation and triple band-notch characteristic. Journal of electromagnetic Waves and Applications. 2017;31(15):1550-65.
[10] Yang F, Rahmat-Samii Y. Microstrip antennas integrated with electromagnetic band-gap (EBG) structures: A low mutual coupling design for array applications. IEEE transactions on antennas and propagation. 2003;51(10):2936-46.
[11] Fu Y, Yuan N. Elimination of scan blindness in phased array of microstrip patches using electromagnetic bandgap materials. IEEE Antennas and Wireless Propagation Letters. 2004;3:63-5.
[12] Lim JS, Kim CS, Ahn D, Jeong YC, Nam S. Design of low-pass filters using defected ground structure. IEEE transactions on microwave theory and techniques. 2005;53(8):2539-45.
[13] Hou DB, Xiao S, Wang BZ, Jiang L, Wang J, Hong W. Elimination of scan blindness with compact defected ground structures in microstrip phased array. IET microwaves, antennas & propagation. 2009;3(2):269-75.
[14] Vazquez C, Hotopan G, Ver Hoeye S, Fernandez M, Herran L, Las-Heras F. Defected ground structure for coupling reduction between probe fed microstrip antenna elements. PIERS Proc, Cambridge, USA. 2010.
[15] Wei K, Li J, Wang L, Xing Z, Xu R. S-shaped periodic defected ground structures to reduce microstrip antenna array mutual coupling. Electronics Letters. 2016;52(15):1288-90.
[16] Luo CM, Hong JS, Zhong LL. Isolation enhancement of a very compact UWB-MIMO slot antenna with two defected ground structures. IEEE Antennas and Wireless Propagation Letters. 2015;14:1766-9.
[17] Anitha R, Sarin V, Mohanan P, Vasudevan K. Enhanced isolation with defected ground structure in MIMO antenna. Electronics letters. 2014;50(24):1784-6.
[18] Sharawi MS, Numan AB, Khan MU, Aloi DN. A dual-element dual-band MIMO antenna system with enhanced isolation for mobile terminals. IEEE antennas and wireless propagation letters. 2012;11:1006-9.
[19] Ren J, Hu W, Yin Y, Fan R. Compact printed MIMO antenna for UWB applications. IEEE antennas and wireless propagation letters. 2014;13:1517-20.
[20] Chen YS, Chang CP. Design of a four-element multiple-input–multiple-output antenna for compact long-term evolution small-cell base stations. IET Microwaves, Antennas & Propagation. 2016;10(4):385-92.
[21] Chiu CY, Cheng CH, Murch RD, Rowell CR. Reduction of mutual coupling between closely-packed antenna elements. IEEE transactions on antennas and propagation. 2007;55(6):1732-8.
[22] Kumar P, Sinha R, Choubey A, Mahto SK. A Novel Metamaterial Electromagnetic Band Gap (MM-EBG) Isolator to Reduce Mutual Coupling in Low-Profile MIMO Antenna. Journal of Electronic Materials. 2021:1-9.
[23] Singh AK, Mahto SK, Sinha R. Compact super-wideband MIMO antenna with improved isolation for wireless communications. Frequenz. 2021.
[24] Kumar, Praveen, et al. "A miniaturized rectangular shape narrowband MIMO antenna with reduced mutual coupling for C-band applications." Journal of Electromagnetic Waves and Applications (2022): 1-14.
[25] Iqbal A, Saraereh OA, Ahmad AW, Bashir S. Mutual coupling reduction using F-shaped stubs in UWB-MIMO antenna. IEEE access. 2017;6:2755-9.
[26] Zhao A, Ren Z. Wideband MIMO antenna systems based on coupled-loop antenna for 5G N77/N78/N79 applications in mobile terminals. IEEE Access. 2019;7:93761-71.
[27] Varshney G, Singh R, Pandey VS, Yaduvanshi RS. Circularly polarized two-port MIMO dielectric resonator antenna. Progress In Electromagnetics Research M. 2020;91:19-28.
[28] Adam I, Yasin MNM, Ramli N, Jusoh M, Rahim HA, Latef TBA, et al. Mutual coupling reduction of a wideband circularly polarized microstrip MIMO antenna. IEEE Access. 2019;7:97838-45.
[29] Khan I, Wu Q, Ullah I, Rahman SU, Ullah H, Zhang K. Designed Circularly Polarized Two-Port Microstrip MIMO Antenna for WLAN Applications. Applied Sciences. 2022;12(3):1068.
[30] Sharma K, Pandey GP. Two port compact MIMO antenna for ISM band applications. Progress In Electromagnetics Research C. 2020; 100:173-85.